Available online at www.sciencedirect.com
SCIENCE DIRECT®
Journal of Computational Physics 205 (2005) 737–754
JOURNAL OF COMPUTATIONAL PHYSICS
www.elsevier.com/locate/jcp

Symbolic implicit Monte Carlo radiation transport in the difference formulation: a piecewise constant discretization ☆

Eugene D. Brooks III *, Michael Scott McKinley, Frank Daffin, Abraham Szöke

Lawrence Livermore National Laboratory, University of California, P.O. Box 808, Livermore, CA 94550, USA

Received 3 June 2004; received in revised form 22 October 2004; accepted 26 November 2004
Available online 21 January 2005

Abstract

The equations of radiation transport for thermal photons are notoriously difficult to solve in thick media without resorting to asymptotic approximations such as the diffusion limit. One source of this difficulty is that in thick, absorbing media, thermal emission and absorption are almost completely balanced. A new formulation for thermal radiation transport, called the difference formulation, was recently introduced in order to remove the stiff balance between emission and absorption. In the new formulation, thermal emission is replaced by derivative terms that become small in thick media. It was proposed that the difficulties of solving the transport equation in thick media would be ameliorated by the difference formulation, while preserving full rigor and accuracy of the transport solution in the streaming limit. In this paper, the transport equation is solved by the symbolic implicit Monte Carlo method and comparisons are made between the standard formulation and the difference formulation. The method is easily adapted to the derivative source terms of the difference formulation, and a remarkable reduction in noise is obtained when the difference formulation is applied to problems involving thick media.

Keywords: Difference formulation; Radiation transport; Implicit Monte Carlo

1. Introduction

The transport of thermal photons in thick media is of sufficient importance that substantial effort has been expended in developing both deterministic [1–4] and Monte Carlo [5] methods for its solution. The

☆ This work was performed under the auspices of the US Department of Energy by the University of California, Lawrence Livermore National Laboratory under Contract No. W-7405-Eng-48.
* Corresponding author. Tel.: +1 925 423 7341; fax: +1 925 423 8086.
E-mail address: brooks3@llnl.gov (E.D. Brooks).

0021-9991/$ - see front matter © 2004 Elsevier Inc. All rights reserved.
doi:10.1016/j.jcp.2004.11.026

difficulties associated with thick media have been severe enough to necessitate solving asymptotic approximations, such as the Eddington and diffusion approximations [6], instead of solving the full transport equation.

Asymptotic methods do give the right solution to the transport equation in uniformly thick media, like stellar interiors. Nevertheless, in many problems of interest the medium is a mixture of thick and thin regions; moreover, some regions of interest may be thin for some radiation frequencies and thick for others.

Although a lot of progress has been made in numerical calculations for such complicated systems using asymptotic methods, they suffer from several defects. One such defect is an unphysical energy propagation rate when the method is applied outside its proper domain. This led to the development of ad hoc corrections such as flux limiters [7]. Another defect is that asymptotic methods are unable to satisfy correct boundary conditions. Time honored "fixes" are the Marshak [8] and Mark [9] boundary conditions, but these incorrect boundary conditions distort ubiquitous boundary layers. More importantly, it is difficult to estimate or measure the errors incurred by the approximations. Only an accurate solution of the transport equation is able to eliminate the above defects.

Several hurdles have stood in the way of producing accurate Monte Carlo solutions of the transport equation in thick media. The first is the selection of a Monte Carlo technique that is numerically stable and provides correct treatment of the stiff coupling between the radiation and the material in the thick limit. Several authors have shown that the radiation-matter coupling is properly treated by the symbolic implicit Monte Carlo method (SIMC) [10,11], producing a correct implicit solution of the radiation field and the material temperature at the end of a time step [12], while effective scattering techniques [5,13,14] possess a significant deficiency in this regard.

A second hurdle has been the very significant noise problem, or the equivalent problem of computational efficiency, when Monte Carlo methods are pressed into service for thick systems. The energy is emitted in a zone uniformly, but only particles born within a few mean free paths of a zone boundary have any chance of contributing to the flux across the boundary. Most of the emitted particles are absorbed within the same zone and serve only to compute the equilibrium values of the radiation intensity and temperature in that zone. This situation for the Monte Carlo method, when applied to thermal photon transport, has been a source of frustration for a long time. The local equilibrium value of the radiation intensity in the thick limit is, of course, the black-body field for the given local temperature. One would prefer not to waste a lot of processing power computing it.

In earlier work [15], some of the authors proposed a new formulation for the transport of thermal photons, referred to as the *difference formulation*. In this scheme, the transport equation is transformed by considering a new field that is the deviation of the local intensity from the local equilibrium intensity. The result of the transformation is to remove the thermal emission source from the transport equation, replacing it with derivative sources that are small in the thick limit. A reasonable conjecture would be that, in the Monte Carlo solution for the transport of the difference field, a significant reduction in noise would result.

In this paper, we demonstrate the validity of this conjecture for the transport of thermal photons. We find that, by employing the difference formulation in a Monte Carlo environment, the effective gain in computational efficiency as compared to the standard formulation increases quadratically with the optical thickness of the problem. The advantage in computational efficiency appears in all portions of a problem where the temperature varies relatively smoothly in space and time and, thereby, the smallness of the source terms is preserved. We describe our Monte Carlo implementation in slab geometry and compare the accuracy and performance for the two formulations for transport.

In optically thick regions, numerical transport methods are usually applied with zone sizes that are much larger than the mean free path of a photon. A low-order discretization, that keeps the temperature and the opacity of the medium constant in each cell, does not yield the correct diffusion limit under such conditions. This "teleportation" effect was discussed in a previous paper [14]. Its deleterious effect can be reduced by using a heuristic known as tilting [16]. Methods that produce a correct solution in the diffusion limit have

generated significant interest in recent years. Deterministic transport techniques which have the diffusion limit [17,18] necessarily go beyond the approximation where the zones have constant values of density, opacity and temperature. In this paper, we restrict ourselves to piecewise constant treatment of the material temperature and therefore we would *not* obtain the proper diffusion limit if the zone sizes were much larger than the photon mean free path. In the present paper we use fine zones and sidestep the issue. We intend to address this deficiency in future work using the methods of [19].

The rest of this paper is organized as follows: In Section 2, we briefly review both the standard and the difference formulation for thermal photon transport in slab geometry, without scattering. A more detailed description of the difference formulation, including scattering, can be found in [15]. In Section 3, we describe the SIMC method employed with a focus on how the implementation differs for the two formulations of transport. Correct frequency sampling of the source terms in the difference formulation requires an extension of the relatively mature techniques used to sample the Planck spectrum [20]. This is discussed in Appendix A. We examine the results of test problems that serve as our basis of comparison for the two transport formulations in Section 4. We end with a discussion in Section 5.

2. Radiation transport in local thermodynamic equilibrium

We review the time and frequency dependent transport of photons in local thermodynamic equilibrium (LTE), without physical scattering, in the standard formulation as well as in the difference formulation. For simplicity we restrict the derivation to a static medium and slab geometry. Scattering is treated identically in the two formulations and we are, therefore, less interested in examining problems with scattering. We examine problems with gray opacities and, in addition, simple frequency dependent opacities where there is a precipitous drop in opacity at higher frequencies. We also consider a temperature dependent specific heat, effectively linearizing the problem, in order to compare our Monte Carlo treatment of the difference formulation to an available analytic solution [21], valid in the diffusion limit.

2.1. Standard formulation

The transport equation describes the propagation of the radiation field in terms of the specific intensity, $I(\mathbf{x},t;\nu;\mathbf{\Omega})$, where $\mathbf{x},t$ are the space and time variables, ν is the radiation frequency and the unit vector $\mathbf{\Omega}$ points in the direction of propagation. The specific intensity is expressed, as usual, in terms of [power/(unit area × unit solid angle × unit frequency interval)]. Using spherical coordinates for the direction of propagation, $\mathbf{\Omega}$, the specific intensity can be written as $I(\mathbf{x},t;\nu;\theta,\phi)$ with the differential of the solid angle $\mathrm{d}\mathbf{\Omega} = \mathrm{d}\mu\,\mathrm{d}\phi$, where $\mu = \cos\theta$.

In slab geometry the radiation field is symmetric around the direction perpendicular to the slab, chosen as the positive x direction. The radiation field is then independent of ϕ, and we transform the remaining angular coordinate from θ to $\mu = \cos\theta$, defining $I(x,t;\nu;\mu) := I(\mathbf{x},t;\nu;\cos\theta,\phi)$, assumed to be independent of ϕ.

The transport equation, in slab geometry and LTE, is then

$$\frac{1}{c}\frac{\partial I(x,t;\nu;\mu)}{\partial t} + \mu\frac{\partial I(x,t;\nu;\mu)}{\partial x} = -\sigma'_{\mathrm{a}}(\nu,T(x,t))[I(x,t;\nu;\mu) - B(\nu,T(x,t))], \tag{1}$$

where $B(\nu,T)$ is the thermal (Planck) distribution at the material temperature, $T(x,t)$, and c is the speed of light. The absorption coefficient, σ'_{a}, is assumed to be corrected for stimulated emission. The specific intensity is related to the photon number distribution function $f(x,t;\nu;\mu)$ by

$$I(x,t;\nu;\mu) = ch\nu f(x,t;\nu;\mu), \tag{2}$$

where $h\nu$ is the photon energy. In Eq. (1), all the variables, I, σ'_a, and B, are functions of the independent variables, $(x,t;\nu;\mu)$ and/or $T(x,t)$. In the following, the independent variables will mostly be suppressed.

The emission function,

$$B(\nu, T) = \frac{2h\nu^3}{c^2}\left(e^{h\nu/kT} - 1\right)^{-1}, \tag{3}$$

can be expressed in terms of a "reduced" frequency distribution function, $b(\nu,T)$,

$$B(\nu, T) = \frac{caT^4}{4\pi} b(\nu, T), \tag{4}$$

where a is the radiation constant. The advantages of using the reduced frequency distribution function are that the strong temperature dependence of thermal emission is factored out by the T^4 term, and that its frequency integral is independent of temperature,

$$\int_0^\infty d\nu\, b(\nu, T) = 1. \tag{5}$$

In slab geometry, the interaction of radiation with matter is expressed by the conservation law

$$\frac{\partial E_{\text{mat}}}{\partial t} = 2\pi \int_0^\infty d\nu \int_{-1}^1 d\mu \sigma'_a [I - B(\nu, T)] + G, \tag{6}$$

where E_{mat} is the energy per unit volume of the material and G is a volume source of energy. The change in energy of the material is related to the change in temperature by its density times the specific heat, ρc_v, which may itself be a function of temperature

$$dE_{\text{mat}} = \rho c_v\, dT. \tag{7}$$

In general, the resulting system of equations is non-linear with the material properties such as opacity and specific heat represented in tabular form. For real problems of interest numerical solution has been our only viable approach.

2.2. The difference formulation

Noting that the solution to the transport equation approaches $B(\nu,T(x,t))$ in the limiting case of a thick system, and that the term I–B occurs in both the transport equation and the equation for energy conservation, we define a difference intensity

$$D(\mathbf{x}, t; \nu; \boldsymbol{\Omega}) := I(\mathbf{x}, t; \nu; \boldsymbol{\Omega}) - B(\nu, T(\mathbf{x}, t)) \tag{8}$$

and, analogously, in slab geometry

$$D(x, t; \nu; \mu) := I(x, t; \nu; \mu) - B(\nu, T(x, t)). \tag{9}$$

We now subtract $(1/c)(\partial B/\partial t) + \mu(\partial B/\partial x)$ from both sides of Eq. (1),

$$\frac{1}{c}\frac{\partial D(x,t;\nu;\mu)}{\partial t} + \mu\frac{\partial D(x,t;\nu;\mu)}{\partial x} = -\sigma'_a(\nu, T(x,t))D(x,t;\nu;\mu) - \frac{1}{c}\frac{\partial B(\nu, T(x,t))}{\partial t} - \mu\frac{\partial B(\nu, T(x,t))}{\partial x}, \tag{10}$$

identifying the last two terms as sources for the transformed equation.

The interaction of radiation with matter is transformed to

$$\frac{\partial E_{\text{mat}}}{\partial t} = 2\pi \int_0^\infty d\nu \int_{-1}^1 d\mu\, \sigma'_a D + G. \tag{11}$$

Let us compare now Eqs. (1) and (10). The propagation and absorption terms of the I field and the D field are the same. In contrast, the source term $\sigma'_a B$ has been traded for the space-time derivative of B. In a thick system with smoothly varying temperatures, the new source terms as well as D are small. The transformed energy equation expressed in terms of the difference field, D, removes the stiff balance between emission and absorption.

An additional impact on numerical solutions stems from the fact that the emission term for the standard formulation contains a factor of σ'_a, adding significant complexity for real materials that have a fine structure representing absorption lines. Because of this, it can be quite difficult to sample the emission spectrum without washing out this level of detail. In comparison, the source terms for the difference formulation are smooth and are accurately sampled using robust methods described in Appendix A. This lack of dependence of the source terms upon material properties makes implementing a code that treats spectral features accurately far less cumbersome, with spectral details appearing only in the absorption terms as particles are tracked and scored.

3. Symbolic implicit Monte Carlo method

We have extended the SIMC method in order to develop a Monte Carlo solution for the difference formulation. Details of the SIMC method are described in [10,11]. The essence of the SIMC method is the factorization of the source terms into a symbolic component, proportional to the unknown T^4 in zone i at the end of the time step, $T_i^4(t_0 + \Delta t)$, and a component specifying the distribution functions for Monte Carlo particle coordinates, $(x,t;\nu;\mu)$, which are handled with explicit sampling. This general theme applies to both formulations of transport discussed in this paper.

In the discussion below, we will sketch the implementation of the SIMC method for the standard formulation as well as for the difference formulation, emphasizing their differences. Since our goal is to understand the basic advantage that the difference formulation offers in thick systems, we do not explore importance sampling methods which would improve things by a small factor for one formulation, or the other. In our Monte Carlo implementation of the two transport formulations we use a piecewise constant treatment of the material temperature, constant as a function of space within each zone. As noted in Section 1, this treatment must be extended if we are to obtain the proper diffusion limit for zones that are optically thick.

In the standard formulation, assuming piecewise constant treatment of the material temperature during the time step, the source term for zone i is written in factored form as

$$\left[\frac{\Delta x_i \Delta t c a T_i^4 \langle \sigma'_a(T_i)\rangle}{2\pi}\right]\left(\frac{1}{2}\frac{1}{\Delta x_i}\frac{1}{\Delta t}\frac{\sigma'_a(T_i)b(\nu,T_i)}{\langle \sigma'_a(T_i)\rangle}\right), \tag{12}$$

where the terms inside the [] are the strength and the terms inside the () are the distribution functions for particle coordinates, $(x,t;\nu;\mu)$; and where $\langle \sigma'_i(T_i)\rangle$ is the Planck average of the absorption cross section, in zone i, given by

$$\langle \sigma'_a(T_i)\rangle = \int_0^\infty d\nu\, \sigma'_a(T_i)b(\nu,T_i). \tag{13}$$

With apologies for the pedantic presentation, the value of which becomes clear when we discuss the source terms for the difference formulation, 1/2 is the distribution function for the direction cosine, $1/\Delta x_i$ is the distribution function for the position coordinate, $1/\Delta t$ is the distribution function for the time coordinate, and $\sigma'_a(T_i)b(\nu,T_i)/\langle \sigma'_a(T_i)\rangle$ is the distribution function of the frequency of the source, evaluated at t_0 within zone i.

The T_i^4 term, having a strong influence on stability, is evaluated at the end of the time step, $t_0 + \Delta t$. This leads to the scoring of the energy depositions by thermally emitted particles in a matrix, identifying the zone from where they were born. The $\langle \sigma'_a(T_i) \rangle$ occurring in the strength term is evaluated at the beginning of the time step because it does not strongly influence stability, and because of the fact that this integral must also be calculated at t_0 in order to handle the frequency distribution of the Monte Carlo particles.

In the difference formulation the source terms are more complicated, but offer the advantage of independence of the detailed optical properties of the material. This independence is a significant advantage in the numerical treatment, removing a source of uncontrolled approximation for real materials. The first complication is that the source is not positive, the solution for the difference field itself only being bounded from below by $-B(v,T(x,t))$. There are two source components,

$$-\frac{1}{c}\frac{\partial B(v,T(x,t))}{\partial t} - \mu\frac{\partial B(v,T(x,t))}{\partial x}, \tag{14}$$

each with different spatial and angular properties. With hindsight, we decompose the sources appropriately for the SIMC treatment

$$-\frac{1}{c}\frac{\partial B}{\partial t} - \mu\frac{\partial B}{\partial x} = \frac{4\pi}{ca}\frac{\partial B}{\partial T^4}\left[-\frac{a}{4\pi}\frac{\partial T^4(x,t)}{\partial t} - \mu\frac{ca}{4\pi}\frac{\partial T^4(x,t)}{\partial x}\right]. \tag{15}$$

It can be shown that $(4\pi/ca)(\partial B/\partial T^4)$ is a frequency distribution function, it being positive everywhere and having unit integral over frequency. We use a discretized form of the derivative for our purposes. Accordingly, we define

$$f(v,T_1,T_2) = \frac{T_1^4 b(v,T_1) - T_2^4 b(v,T_2)}{T_1^4 - T_2^4}. \tag{16}$$

The temperatures T_1 and T_2 are either the temperatures at the beginning and end of the time step, or are the temperatures on the left and right hand side of a zone interface. It yields the reduced Planck distribution, $b(v,T)$, when one of the temperatures is zero. It must be treated with care when the difference in temperatures is small if a correct spectrum is to be obtained. We discuss this, along with our sampling techniques for $f(v,T_1,T_2)$, in Appendix A.

In finite difference form, the $\partial B/\partial t$ component of the source terms within a time step Δt is

$$\frac{a}{4\pi}\frac{T_i^4(t_0) - T_i^4(t_0+\Delta t)}{\Delta t} f(v,T(t_0),T(t_0+\Delta t)). \tag{17}$$

This source term can be factored into a strength term and distribution functions for particle coordinates just as was the case for the standard formulation; the key difference being that we do not have to multiply and divide by Δt, and that the $T(t_0 + \Delta t)$ occurring in the frequency distribution function must be extrapolated from the prior time step.

The $\partial B/\partial x$ source term is a little more complicated, and in this case the factorization into strength and distribution functions is perhaps more useful. Because of the piecewise constant treatment of the material temperature, the derivative is zero except on the boundaries between zones, and at the exterior boundaries of the problem.

An additional property of this source, arising from the factor μ, is that its angular integral is zero, at any point in space and time. We choose to satisfy this conservation law by sampling correlated particle pairs in $\pm\mu$ directions, with equal and opposite weights, although other schemes are possible for the angular sampling and might, in fact, be preferred.

The positive μ portion of this source during a time step Δt, separated into strength and distribution functions, is

$$\left[\Delta t \frac{ca}{8\pi}\left(T^4_{\mathrm{l}(j)}(t_0+\Delta t) - T^4_{\mathrm{r}(j)}(t_0+\Delta t)\right)\right]\left((2\mu)\delta(x-x_j)\frac{1}{\Delta t}f\left(v, T_{\mathrm{l}(j)}(t_0), T_{\mathrm{r}(j)}(t_0)\right)\right), \tag{18}$$

where $T_{\mathrm{l}(j)}$ refers to the temperature on the left side of *interface j* and $T_{\mathrm{r}(j)}$ refers to the temperature on the right side, with x_j being the position of the interface and δ the Dirac delta function.

As before, the strength of the source term to be divided among the source particles is enclosed in the []. The distribution functions for particle coordinates, $(x,t;v;\mu)$, are enclosed in the ( ). The angular distribution function is (2μ), particles are sourced only on the interface located at x_j, particles are sampled uniformly across the time step, and the frequency distribution function is $f(v,T_{\mathrm{l}(j)},T_{\mathrm{r}(j)})$, evaluated at the beginning of the time step. As noted earlier, for each particle sampled in the $+\mu$ direction a particle of equal and opposite weight is emitted in the $-\mu$ direction with otherwise identical particle coordinates.

Fixed temperature boundary conditions are handled by using the appropriately prescribed temperature. A vacuum boundary condition is handled with a prescribed temperature of zero, providing $D = I$ on the problem exterior. In fact, the outgoing source for the last interface to problem exterior need not be sampled via Monte Carlo, it only serves to introduce noise in the "output" from the surface and can be scored deterministically.

The non-linear system to solve in order to update the temperature is obtained by integrating Eq. (6) for the standard formulation, or Eq. (11) for the difference formulation, using Eq. (7) to relate the change in energy to the change in temperature. The scoring of thermally emitted particles yields a banded matrix in the space of zone indices where the bandwidth is controlled by $c\Delta t$, and also by the opacity because we remove particles that have been attenuated to less than 10^{-6} times their birth weight. The non-linear system is solved by Newton–Raphson iteration after the Monte Carlo particles reach census. The actual value of $T^4_i(t_0+\Delta t)$ is then substituted, thereby converting all census particles to known weights in order to prepare for the next time step. The basic scheme is the same for both the standard and the difference formulations. Only the details of the scoring function are different. In the standard formulation, the unknown factor is $T^4_i(t_0+\Delta t)$. In the difference formulation, the unknown factors are $(T^4_i(t_0) - T^4_i(t_0+\Delta t))$, with i referring to zones, and $(T^4_{\mathrm{l}(j)}(t_0+\Delta t) - T^4_{\mathrm{r}(j)}(t_0+\Delta t))$, with j referring to interfaces, for particles produced by the $\partial B/\partial t$ and the $\partial B/\partial x$ source terms, respectively. [1]

4. Test problems

A variety of test problems have been examined in order to evaluate the computational efficiency and accuracy of the difference formulation, employing the SIMC method described earlier. Our goal is to analyze some simple situations that indicate the potential impact of the difference formulation in more complex physics environments. The key issues are accuracy and efficiency for both thick and thin media – specifically the frequent occurrence of media which are thick at one frequency while being thin at others. In addition to comparing the Monte Carlo solution of the two formulations of transport, we compare them to available semi-analytic solutions.

4.1. Behavior of a finite slab heated from the outside

The most basic test of a thermal transport algorithm is whether it correctly approaches the steady-state solution for a finite slab immersed in a heat bath with different temperatures on either side. At the coarsest level, in thick media, the steady-state solution of the material temperature, raised to the fourth power, is a

[1] In the $\partial B/\partial t$ term, the temperature is handled in the form $(T^4_i(t_0) - T^4_i(t_0+\Delta t))$, both to simplify the code and to avoid the noise and possible numerical difficulties associated with two independent particle weights when tracking Monte Carlo particles.

straight line when plotted as a function of optical depth. Deviations from a straight line are indicative of boundary layers when they occur within a mean free path or so of a surface, but otherwise they indicate serious problems in the numerical solution. Teleportation errors result in a wrong slope and cause curvature in the interior solution [14]; this is the reason why we limit zone thickness to one mean free path in our piecewise constant treatment of the material temperature.

The time dependent approach to steady state offers the opportunity to check the correctness of the implementation of interior source terms as well as initial and boundary conditions. That the steady-state temperature is independent of time step size, reflecting implicit behavior of the time integration, can also be checked. When the spectrum of the radiation field is examined, even for a gray opacity, the correctness of the frequency sampling algorithm can be checked. Agreement between the standard and difference formulation is non-trivial due to the different nature of their source terms. A detailed description of all the checks described above is beyond the scope of this paper, but they have been carried out.

In the presentation of our computational results below, we provide a clear demonstration of rigorous agreement between the two formulations for transport, in terms of their approach to steady state, along with a measure of the increase in computational efficiency for the difference formulation. The magnitude of this increase in computational efficiency, in the form of greatly reduced Monte Carlo noise as the optical thickness of the problem is increased, is somewhat surprising even to the authors who were prospecting for it.

In the first set of simulations, we consider a finite slab heated from the left side, with an open boundary on the right, allowing the radiation flowing through the slab to enter free space. The slab is composed of a uniform, static material having a frequency-independent (gray) opacity and constant specific heat. We calculate the time dependence of the temperature and of the radiation field after a 1 keV black-body source on the left side of the slab is turned on at time $t = 0$ (1 keV $\approx 1.2 \times 10^7$ K).

During the time dependent execution of the problem, a thermal wave, also known as a Marshak wave, sweeps the problem domain, and the solution then approaches steady state. Under conditions where the Monte Carlo portion of the code dominates execution time, we compare the solutions provided by the two formulations. The relative noise for identical problem run times provides a measure of computational efficiency.

For four instances of this problem, the slab is composed of a uniform material having a frequency independent (gray) opacity of 0.1, 1, 10, and 100 mean free paths per cm, respectively. The specific heat of the material is a constant 0.1 jerk/(keV cm^3), where jerk is an energy unit (1 jerk = 10^{16} ergs), and temperature is measured in energy units of $kT = 1$ keV. The slab is initially at a temperature of 0.01 keV, with the radiation field being a Planckian in equilibrium with this temperature. The slab is 10 cm thick, so the four opacities correspond to total optical depths of 1, 10, 100 and 1000 mean free paths.

All four problems used a time step of 0.2 sh, where 1 sh = 10^{-8} s. The problems 1 and 10 mean free paths thick were run to 20 sh to equilibrate. The problem 100 mean free paths thick was run to 40 sh in order to approach steady state. The problem 1000 mean free paths thick moved very slowly due to the diffusive nature of the solution, requiring 320 sh in order to suitably approach steady state.

The problems 1 and 10 mean free paths thick employed 20 zones, while the thicker problems employed zones one mean free path thick in order to prevent teleportation error from influencing the results and to prevent anomalous performance results for the difference formulation. Zones of equal thickness were used everywhere. Geometric zoning has a role in reducing computational cost only if a piecewise linear treatment of material properties is available to keep teleportation error under control [19].

Note that the Monte Carlo solution for the two transport formulations have entirely different requirements for spatial importance sampling if uniform statistical noise, as a function of position, is to be obtained. In the standard formulation most of the computational effort is spent computing the balance between emission and absorption that produces the local equilibrium black-body field. As a result, a scheme that samples particles with uniform density in space produces a relatively flat statistical noise profile across

the slab. During each time step, the source particles for the standard formulation are uniformly divided among the zones, which are of equal size.

The statistical properties of the Monte Carlo solution for the difference formulation are in sharp contrast to this. For thicker problems the statistical noise for the difference formulation is small near the hot side and increases rapidly towards the cold boundary. Suitable importance sampling would flatten out this growth in noise. An exposition of this issue is beyond the scope of this paper. In our tests we sampled an equal number of $\partial B/\partial t$ particles across the zones, and the same number of $\partial B/\partial x$ particle pairs across the interfaces.

In the examples shown in this paper, then, the unit of source sampling for the difference formulation is one $\partial B/\partial t$ particle and one $\partial B/\partial x$ particle pair, for each zone or zone interface, respectively. We have not attempted to tune the ratio between $\partial B/\partial t$ and $\partial B/\partial x$ source particles, nor have we attempted to tune the relative importance of source sampling across the volume of the problem. In the standard formulation the unit of source sampling is one thermally emitted particle per zone. The total number of source particles for runs employing the standard formulation, and runs involving the difference formulation, is adjusted so that the execution time is dominated by the Monte Carlo, and set so that the total run time for the two formulations is identical.

In Fig. 1(a), we show the steady-state solution for the material temperature as a function of position in the slab that is one mean free path thick. The average of 100 randomly seeded runs using the standard formulation, and the difference formulation, is shown. The two formulations are in good agreement. The standard deviation of the results for the standard formulation as well as for the difference formulation, both multiplied by 400, are plotted. Comparing standard deviations for the equal problem run times, the difference formulation is outperforming the standard formulation, except near the surface on the right hand side. Note that the thickness of each zone is only 0.05 optical depths.

In Fig. 1(b), we show the results for a slab that is 10 mean free paths thick. Again, we obtain excellent agreement between the two formulations, comparing the equilibrium material temperature. In order to display the standard deviation of the temperature for the two formulations on the same plot, we apply a scale factor of 100 for the standard formulation and 1000 for the difference formulation. A trend of growth of the standard deviation for the difference formulation, as the temperature gradient increases in the slab from left to right, is becoming apparent.

In Fig. 1(c), we show the results for a slab that is 100 mean free paths thick. There are 100 zones in this problem in order to minimize teleportation error, with every fifth point plotted using a symbol. The other points are included in the solid lines drawn. We apply a scale factor of 20 to the standard deviation for the standard formulation, and a scale factor of 1000 to the standard deviation for the difference formulation. The trend of growth in the standard deviation for the difference formulation as one traverses the slab from left to right is now quite clear, but the overall computational advantage for the difference formulation has increased with optical depth.

In Fig. 1(d), we show the results for a slab that is 1000 mean free paths thick. There are 1000 zones in this problem, a requirement to avoid significant teleportation error, with every 50th zone plotted using a symbol. The disagreement between the two formulations appearing towards the left side of the slab is due to statistical fluctuations in the standard formulation. The computational advantage of the difference formulation has continued to increase as the opacity is increased.

Evidence of the scaling behavior of the computational advantage of the difference formulation is shown in Fig. 2. The figure illustrates the computational advantage of the difference formulation when calculating the material temperature, as a function of position, for the four optical thicknesses shown in Fig. 1. As indicated earlier, the particle counts in the Monte Carlo runs for the two formulations are set so that the Monte Carlo dominated run times are the same. Under this condition, the computational advantage is the square of the ratio of the standard deviations of the random sample of runs completed for each formulation,

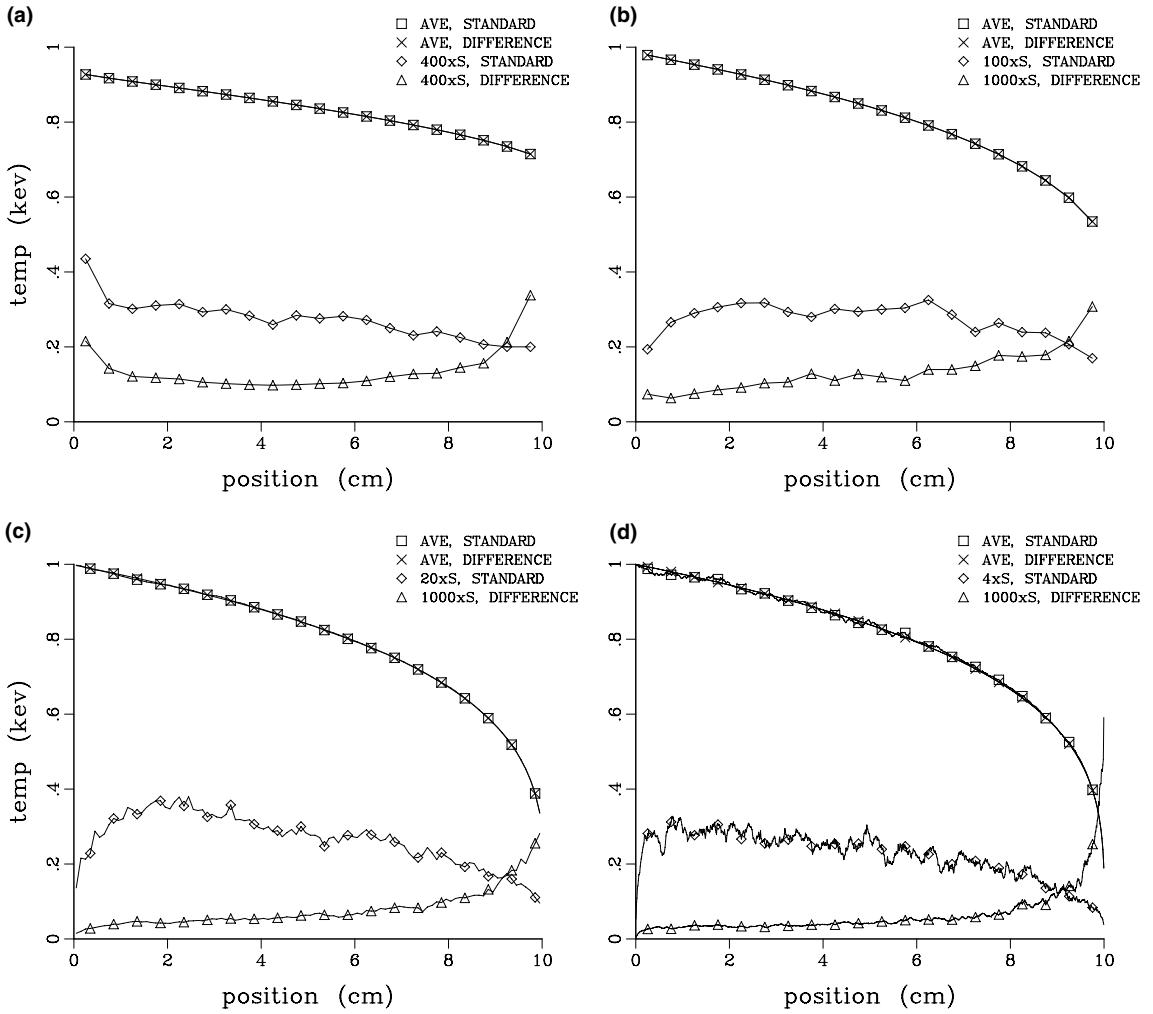

Fig. 1. Temperature distribution in a slab in steady state. The slab is heated from the left by a 1 keV black body, and it radiates freely on the right. The total optical depth (OD) of the slab is 1 in (a), 10 in (b), 100 in (c) and 1000 in (d). The standard deviation of the standard formulation is denoted by diamonds and that of the difference formulation by triangles. Note the change in their relative scale with optical depth. The noise in the standard formulation increases dramatically with optical depth, while in the difference formulation it does not.

plotted in Fig. 1(a)–(d). The computational advantage scales roughly as the square of the optical thickness of the problem.

In Fig. 3, we show the penetration of a thermal wave into a slab 1000 mean free paths thick at 40 sh, for a single problem run with the same parameters as in Fig. 1(d). The solution shown is fully converged as a function of time step and zone size. This figure visibly illustrates the gains that the difference formulation provides.

The reader may note that the result for the difference formulation has the appearance of smooth curve. The $1/\sqrt{N}$ noise behavior that is typical of a Monte Carlo solution is present, it is just that the amplitude of the noise is too small to be resolved in the figure.

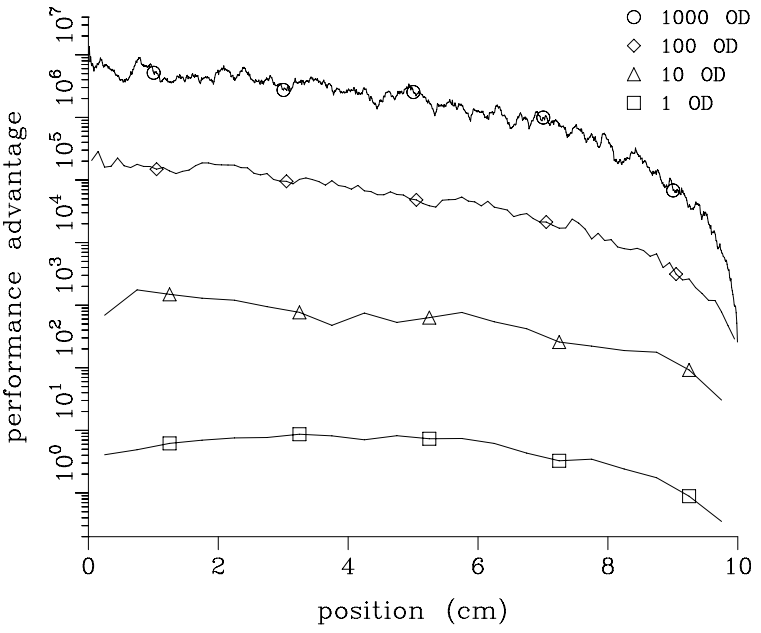

Fig. 2. The relative computational advantage of the difference formulation compared to that of the standard formulation, plotted as a function of position for various optical depths of the slab. In the 1 OD case, each zone is only 1/20 OD thick, nevertheless, the difference formulation is better than the standard one except near the surface of the slab on the right hand side. There is a sharp decrease in computational advantage where the temperature gradient is large. This could easily have been remedied by spatial importance sampling of the source particles.

4.2. Comparison to analytic diffusion solution for a linearized problem

In order to check the correctness of our numerical implementation, we have compared our results with the diffusion solution appearing in [21]. This solution requires that the material energy take the form

$$E_{\text{mat}} = \frac{\alpha T^4}{4}, \tag{19}$$

or, equivalently, that the specific heat take the form

$$\frac{\partial E_{\text{mat}}}{\partial T} = \alpha T^3, \tag{20}$$

where α is a specified constant. This form for the material energy results in equations linear in T^4, allowing an analytic solution. The resulting analytic solution can then be used to check for the correct convergent behavior in our numerical simulation. The behavior of the specific heat at $T = 0$, however, makes the numerical calculation quite fragile unless the code itself is transformed to handle things in the linearized form. To some extent, this defeats the purpose of checking the original code, much of which had to be modified to accommodate the linearized form.

For this test problem, α and the absorption cross section were chosen so that the values in the tables of analytical results appearing in [21] could be used directly. In Fig. 4 we plot the material temperature produced by our Monte Carlo solution of the standard and difference formulations, along with data from Su and Olson's analytical solution corresponding to a late time, their $\tau = 10$. We obtain good agreement where analytical data are available. This is expected because for $\tau = 10$ the diffusion approximation assumed by Su

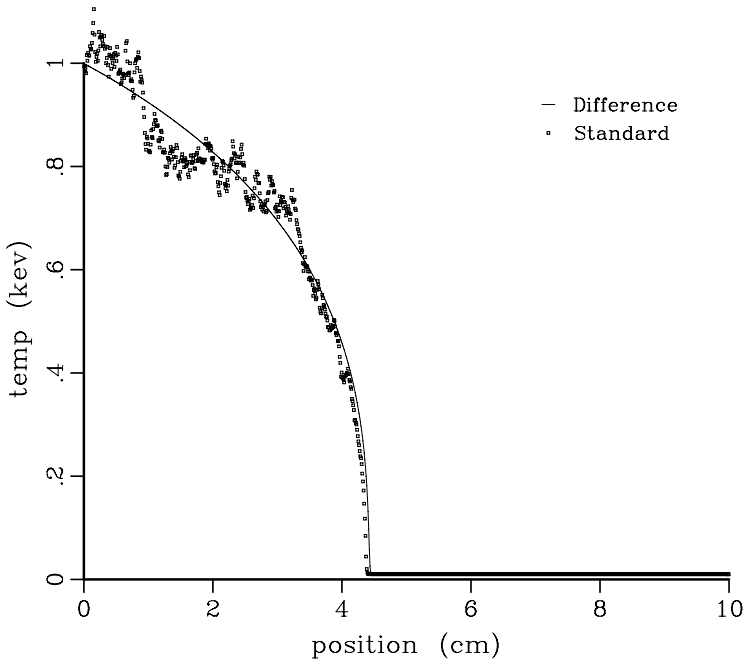

Fig. 3. Thermal wave (Marshak wave) penetrating a uniform, gray slab of 1000 OD at an early time, 40 sh. The standard formulation gives a noisy temperature profile whereas that of the difference formulation is many orders of magnitude smoother. The slight difference in the position of the leading edge is a statistical fluctuation for the standard formulation.

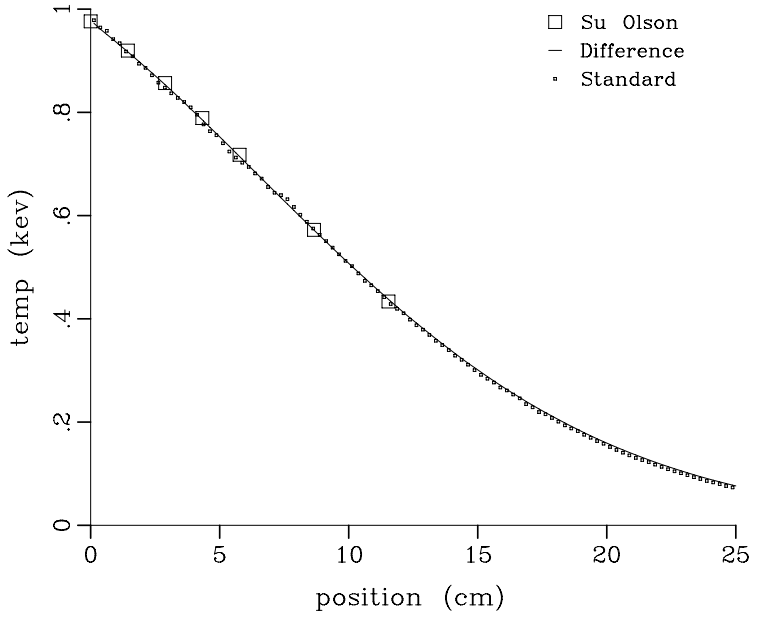

Fig. 4. Temperature distribution in the Su and Olson problem [21] at a late time $\tau = 10$. There is excellent agreement of the calculations with analytic results.

and Olson is valid. In Fig. 5 we plot the material temperature for the same problem along with data from Su and Olson's analytical solution for $\tau = 0.01$. Not surprisingly, there is sharp disagreement between the diffusion solution and the fully overlapped and converged Monte Carlo transport solutions for the standard and the difference formulations. Here the fundamental limitation is the speed of light; it is fully respected by the transport solution but ignored by the diffusion solution, unless ad-hoc corrections are used.

4.3. Time dependent Marshak wave problem, with a non-trivial opacity

Our Monte Carlo solutions of the standard and difference formulations of transport fully implement the details of the thermal frequency spectrum; the spectral properties of the derivative sources make the agreement between the two formulations non-trivial even in the case of a gray opacity. Once the spectral sampling of the source terms in the difference formulation is done correctly, as described in Appendix A, there is no more to be done for the correct treatment of a frequency dependent opacity in the difference formulation other than to use the correct absorption cross section for a given Monte Carlo particle. The accuracy of the treatment of the frequency dependent cross section is as good as the cross section itself.

The emission term for the standard formulation, on the other hand, appears as $\sigma'_a B$. In the most general case, it must be numerically integrated across the frequency group structure in each zone at the start of each time step. This requirement provides another place where numerical errors must be controlled in the implementation of the standard formulation.

We now turn to a relatively simple frequency dependent opacity: one that is 1000 mean free paths for the slab for frequencies below 1 keV and 10 mean free paths for the slab for frequencies above 1 keV. This corresponds, roughly, to the precipitous drop in opacity as a function of frequency that can occur in real materials. The portion of the emitted spectrum below 1 keV is strongly re-absorbed, while the portion of the

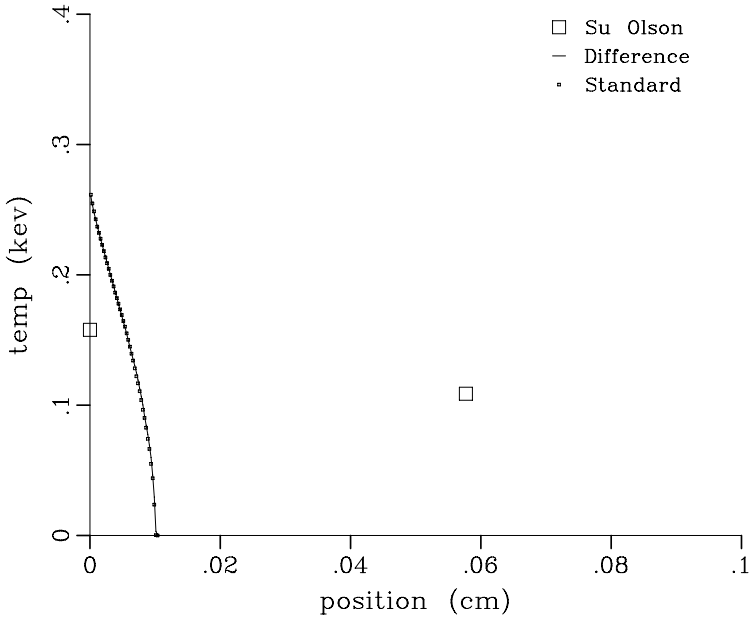

Fig. 5. Temperature distribution in the Su and Olson problem [21] at an early time $\tau = 0.01$. The transport solution is limited by the speed of light, that is 1 in the units of τ. Note that there is no significant spreading of the radiation front at the leading edge of the thermal wave.

emitted spectrum above 1 keV encounters a lower opacity and transports freely. This is a difficult non-linear problem because, as the trapped radiation heats the material, the Planckian emission spectrum moves towards higher frequencies where radiation flows freely.

In Fig. 6, we show the material temperature for one instance of this problem at $t = 1$ sh, a time where the thermal wave is still propagating through the slab. As before, the standard formulation is the one exhibiting a high level of statistical noise. Note, however, that this noise disappears in the "foot" of the advancing thermal wave. This feature is produced by high-frequency photons that encounter a lower material opacity, and therefore produce less noise in the standard formulation.

5. Discussion

The SIMC method [10] is an attractive framework for the calculation of radiation transport in complex media and geometries; it provides a basis for accurate and stable numerical schemes [11,12]. In this paper, we have demonstrated that the difference formulation [15] is eminently suitable for numerical calculations of radiation transport in LTE, employing the SIMC technique.

Our theoretical expectations were that the standard formulation would be better for thin media, while the difference formulation would be advantageous in thick media. We have demonstrated that the difference formulation, when employing the SIMC technique, offers significant noise reduction for thick systems, with its computational advantage scaling like the square of the opacity. The expected cross-over vis-a-vis the standard formulation occurs only for very thin systems, thin enough that the difference formulation might become a panacea for the Monte Carlo treatment of thermal radiation transport in practical problems.

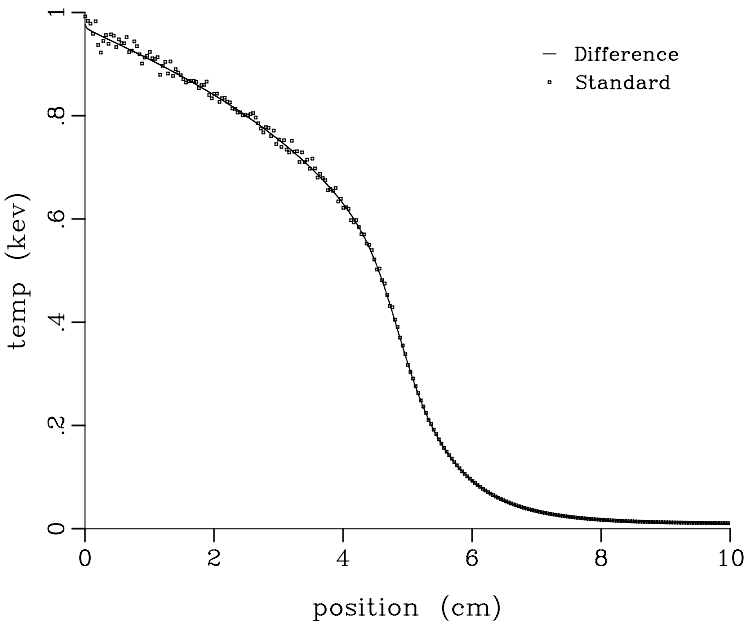

Fig. 6. Thermal wave penetrating a uniform slab, shown at a time $t = 1$ sh. The optical thickness of the slab below 1 keV is 1000 mean free paths, but there is a precipitous drop in opacity by a factor of 100 above 1 keV. The long "foot" of the thermal wave stems from high frequency photons that penetrate deeply.

The character of the source terms is very different in the standard and the difference formulations: thermal emission in the former is replaced by derivative source terms in the latter. Therefore a key issue for the accuracy and stability of the difference formulation is the successful treatment of the derivative source terms. We have developed efficient, accurate analytic techniques for sampling the frequency spectrum of the source terms for the difference formulation. Frequency sampling in the difference formulation depends only on the space and time derivative of the material temperature, not on its optical properties. This offers a significant advantage for problems with complicated material optical properties. When we implemented the test problem with the step in opacity, the value of this reduction in code complexity became clear. Although the test problems we presented were simple in order to clearly identify the advantages of the difference formulation, extensions to more complex situations do not present conceptual difficulties.

The computational gain for the difference formulation demonstrated in this paper is for the Monte Carlo portion of the problem. In order to obtain implicit treatment of the source terms, the SIMC technique requires the solution of a non-linear system of equations in order to perform the temperature update at the end of the time step. The cost of this can become significant when the number of zones in the problem is large. We used band-limited Gaussian elimination, at the core of a Newton–Raphson solver, in our numerical work on problems with as many as 1000 zones. The bandwidth was limited both by the time step size and by the death of Monte Carlo particles when they became too small, relative to their birth weight. The number of Newton–Raphson iterations does not differ substantially for the two formulations. Multi-dimensional problems with significantly larger numbers of zones will pose a challenge, requiring the use of suitable iterative solution techniques. Nonetheless, we believe that the demonstrated noise reduction in thick systems will be worth the effort involved.

In our numerical evaluation of the difference formulation, we have employed a piecewise constant discretization for the material temperature. Due to teleportation effects, this discretization does not provide the correct diffusion limit for zone sizes that are large compared to the mean free path of a photon. A piecewise linear treatment of the material temperature is required to remove this defect [19]. In order to obtain a more accurate solution, both the time discretization and the treatment of the frequency spectrum of the emitted photons will have to be improved. These issues will be addressed in future work.

Our test problems have been relative simple, suitable as the first Monte Carlo tests for the difference formulation for thermal radiation transport. It is clear that the spatial importance sampling requirements for the difference formulation are quite different than those for the standard one. It is also the case that improvements such as weight vectors in frequency space and deterministic handling of the spectral output from the interface adjoining free space have a significant impact on noise when spectral information associated with the photon field is desired. The details of these improvements, along with their relative value, depend on the exact nature of the problems being run and the computational results that are desired. They are beyond the scope of this paper.

Relaxing the need for implicit treatment of the source terms was one of the hopes of the authors, given that implicit treatment requires the solution of a non-linear system of equations for each time step. Our experiences in this regard, documented in [22], were made even more difficult by the T^4 term for thermal emission. As a result, we used the fully implicit treatment of the source terms in this work. This issue may be worth revisiting in more complex physics applications where the time step size is limited for reasons outside of transport physics, and might satisfy any time step control requirement for the transport without introducing further constraint.

Finally, we note that our work may open the door to significant improvements in the numerical treatment of more general transport problems and methods. We can envisage application to scattering atmospheres, Comptonisation, [2], etc. Although this paper provides no obvious lessons for deterministic methods, these might also benefit from the smallness of the source terms appearing in the difference formulation, for thick systems.

Acknowledgment

The authors thank Bret Beck for contributing the rejection technique that sampled the two temperature frequency distribution function.

Appendix A. Sampling the frequency probability density function

The frequency probability density function (p.d.f.) was given previously in Eq. (16) as a function of frequency v and two temperatures, T_1 and T_2:

$$f[v, T_1, T_2] = \frac{b(v, T_1)T_1^4 - b(v, T_2)T_2^4}{T_1^4 - T_2^4}. \tag{A.1}$$

Sampling a frequency from this distribution function is not straightforward because there are two limiting cases to deal with. The first occurs when one of the temperatures is zero (or is a vacuum interface). In this event, the p.d.f. turns into a Planckian and is sampled using the method of [20]. The other limiting situation is when the temperatures are close. There, the limit of the p.d.f. as T_2 approaches T_1 must be used, which returns us to the original derivative:

$$\lim_{T_1 \to T_2} \frac{b(v, T_1)T_1^4 - b(v, T_2)T_2^4}{\left(T_1^4 - T_2^4\right)} = \frac{4\pi}{ca}\frac{\partial B(v, T)}{\partial T^4}. \tag{A.2}$$

This may be sampled by expanding B from Eq. (3) and defining $x = hv/kT$ to get a unit-less cumulative density function (c.d.f.) for x:

$$\text{c.d.f.} = \int_0^v \frac{4\pi}{ca}\frac{\partial B(v', T)}{\partial T^4}\mathrm{d}v' = \int_0^v \frac{15}{4\pi^4}\frac{\mathrm{e}^{hv'/kT}h^5v'^4}{\left(\mathrm{e}^{hv'/kT} - 1\right)^2 k^5 T^5}\mathrm{d}v' = \int_0^x \frac{15}{4\pi^4}\frac{x'^4\mathrm{e}^{-x'}}{\left(1 - \mathrm{e}^{-x'}\right)^2}\mathrm{d}x'. \tag{A.3}$$

Multiplying and dividing the integrand by $(1 + \mathrm{e}^{-x}/x^2)$ gives a probability distribution function (p.d.f.) of the form

$$\text{p.d.f.}(x) = [\pi_1 f_1(x) + \pi_2 f_2(x)]h(x), \tag{A.4}$$

where $\pi_1 + \pi_2 = 1$, $\int_0^\infty f_i(x)\mathrm{d}x = 1$, and $x \geqslant 0$. It can be verified that $\pi_1 = 96/97$, $\pi_2 = 1/97$, $f_1 = (1/24)x^4\,\mathrm{e}^{-x}$, $f_2 = 4x^2\,\mathrm{e}^{-2x}$, and $h = [1455x^2]/[16\pi^4(1 - \mathrm{e}^{-x})^2\,(x^2 + \mathrm{e}^{-x})]$.

This may be sampled using a rejection technique [23] with the comparison function being Eq. (A.4), using for $h(x)$ its maximum, $h_{\max}$. Then, x_i is sampled from f_1 with a probability π_1 and from f_2 otherwise. The sample is kept if a random number is less than $h(x_i)/h_{\max}$.

Finally, in the most general case we investigated two options, the first of which is to develop a table look-up method. The reduced frequency distribution function, $b(x)$, was numerically integrated and fitted with a spline in order to construct a table that can be used to quickly compute the c.d.f. corresponding to Eq. (A.1). A Newton–Raphson method is then used to invert the c.d.f.

The second method employs a rejection technique by expanding b in Eq. (A.1) and defining $C = \min(T_1,T_2)/\max(T_1,T_2)$, where (min,max) are the (minimum, maximum) of their arguments and $x = (hv)/(k\,\max(T_1,T_2))$, to rewrite Eq. (A.1) in the form:

$$g(x) = \frac{x^3}{1 - C^4}\left(\frac{1}{\mathrm{e}^x - 1} - \frac{1}{\mathrm{e}^{x/C} - 1}\right), \tag{A.5}$$

where we have left off the normalization that is not required for our purposes.

We observe that a function $f(x)$ defined by

$$f(x) = x^2 e^{-1.5x} + x^3 e^{-ax}; \quad a = 1 - 0.1C \tag{A.6}$$

is easily sampled and satisfies the relation $f(x) \geqslant g(x)$.

The frequency may then be sampled with the following rejection algorithm where r's represent random numbers from 0 to 1:

(1) If $r_1 < 1/[1 - (3 \times 1.5^3)/a^4]$ then goto (2) else goto (3)
(2) Sample $x^2 e^{-1.5x}$: $x = \ln(r_3 r_4 r_5)/1.5$; goto (4)
(3) Sample $x^3 e^{-ax}$: $x = \ln(r_3 r_4 r_5)/a$
(4) If $f(x) \times r_2 > x^3[(e^x - 1)^{-1} - (e^{x/C} - 1)^{-1}]/(1 - C^4)$ then goto (1)
(5) The sampled frequency is $x\frac{k}{h}\max(T_1, T_2)$.

Speed and accuracy were investigated on four different architectures for a variety of C values (ratio of low to high temperature). The accuracy of the Planckian, table lookup and general rejection method appeared to be about the same for $C \leqslant 0.01$. Similarly, the accuracy of the $\partial B/\partial T^4$ limit, table lookup and general rejection method were about the same for $C \geqslant 0.99$.

Execution time depended upon the computer architecture employed, but there were general trends. Each method was sampled 100 million times on each architecture for different values of C. For C below 0.1, the fastest method was the Planckian. The general rejection method was 15% slower and the table lookup was about twice as slow. For C above 0.9, the fastest method was the $\partial B/\partial T^4$ limit. The general rejection method using Eq. (A.5) was about the same speed while the table lookup was about four times slower.

In summary, we use the Planckian method for $C \leqslant 0.01$, $\partial B/\partial T^4$ limit method for $C \geqslant 0.99$ and the general rejection method using Eq. (A.5) otherwise.

References

[1] D. Mihalas, Stellar Atmospheres, Freeman, San Francisco, 1978, pp. 64–71.
[2] John I. Castor, Radiation Hydrodynamics, Cambridge University Press, Cambridge, 2004.
[3] D. Mihalas, B.W. Mihalas, Foundations of Radiation Hydrodynamics, Oxford University Press, New York, 1984.
[4] G.C. Pomraning, The Equations of Radiation Hydrodynamics, Pergamon, Oxford, 1973.
[5] J.A. Fleck Jr., J.D. Cummings, An implicit Monte Carlo scheme for calculating time and frequency dependent radiation transport, J. Comput. Phys. 8 (1971) 313.
[6] E.W. Larsen, G.C. Pomraning, V.C. Badham, Asymptotic analysis of radiative-transfer problems, J. Quant. Spectr. Rad. Transfer 29 (1983) 285.
[7] G.C. Pomraning, Flux limiters and Eddington factors, J. Quant. Spectr. Rad. Transfer 27 (1982) 517–530.
[8] R.E. Marshak, Note on the spherical harmonic method as applied to the Milne problem for a sphere, Phys. Rev. 71 (1947) 443–446.
[9] J.C. Mark, The spherical harmonic method, Technical Report, CRT-340, Atomic Energy of Canada, Ltd., Ontario, 1947.
[10] E.D. Brooks III, Symbolic implicit Monte Carlo, J. Comput. Phys. 82 (1986) 433.
[11] T. N'kaoua, Solution of the nonlinear radiative transfer equations by a fully implicit matrix Monte Carlo method coupled with the Rosseland diffusion equation via domain decomposition, SIAM J. Sci. Stat. Comput. 12 (1991) 505.
[12] J.D. Densmore, E.W. Larsen, Asymptotic equilibrium diffusion analysis of time-dependent Monte Carlo methods for grey radiative transfer, J. Comp. Phys. 199 (2004) 175–204.
[13] L.L. Carter, C.A. Forest, Nonlinear radiation transport simulation with an implicit Monte Carlo method, LA-5038, Los Alamos National Laboratory, 1973 (unpublished).
[14] M.S. McKinley, E.D. Brooks, A. Szoke, Comparison of implicit and symbolic implicit Monte Carlo line transport with frequency weight vector extension, J. Comp. Phys. 189 (2003) 330–349.
[15] A. Szöke, E.D. Brooks III, The transport equation in optically thick media, J. Quant. Spectr. Rad. Transfer 91 (2005) 95–110.
[16] J.A. Fleck, E.H. Canfield, Random walk procedure for improving the computational efficiency of the implicit Monte Carlo method for nonlinear radiation transport, J. Comp. Phys. 54 (1984) 508–523.

[17] J.E. Morel, T.A. Wareing, K. Smith, A linear-discontinuous spatial differencing scheme for S_N radiative transfer calculations, J. Comput. Phys. 128 (1996) 445.
[18] M.L. Adams, P.F. Nowak, Asymptotic analysis of a computational method for time- and frequency-dependent radiative transfer, J. Comput. Phys. 146 (1998) 366.
[19] J.-F. Clouet, G. Samba, Asymptotic diffusion limit of the symbolic Monte-Carlo method for the transport equation, J. Comput. Phys. 195 (2004) 293.
[20] C. Barnett, E. Canfield, Sampling a random variable distributed according to Planck's law, Lawrence Livermore National Laboratory, UCRL-ID-125393 (1970) (unpublished).
[21] B. Su, G.L. Olson, Benchmark results for the non-equilibrium Marshak diffusion problem, J. Quant. Spectr. Rad. Transfer 56 (1996) 337–351.
[22] F. Daffin, M.S. McKinley, E.D. Brooks III, A. Szoke, An evaluation of the difference formulation for photon transport in a two level system, J. Comput. Phys. (in press), Lawrence Livermore National Laboratory, UCRL-JRNL-204366 (2004).
[23] M.H. Kalos, P.A. Whitlock, Monte Carlo Methods, Vol. 1: Basics, John Wiley and Sons, New York, 1986, pp. 61–71.